A technical note on performance of single-dipole and dual-dipole inverse solutions

Vojko Jazbinšek, Rok Hren

Inštitut za matematiko, fiziko in mehaniko

Uvod

- Matematično modeliranje tako izvorov kot prostorskih prevodnikov ostaja eden od nujnih pogojev za kvantitavni opis elektrokardiografskih podatkov.
- Že relativno enostaven model tokovnega dipola v homogenem in izotropnem modelu torza, ki predstavlja srčni tokovni izvor in električne lastnosti človeškega telesa, zahteva numerično računanje zaradi nepravilne oblike telesa.
- V tem prispevku smo izbrali poenostavljen pristop, kjer realistično obliko človeškega telesa zamenjamo s homogeno prevodno kroglo.
- V tem modelu lahko električni potencial, ki izvira iz tokovnega dipola znotraj krogle, izračunamo analitično v poljubni točki znotraj krogle in na njeni površini.

<u>Motivacija:</u> Določiti vpiv izbire merskih mest in merskega šuma na lokalizacijo enojnih in dvojnih dipolnih izvorov.

Postopek:

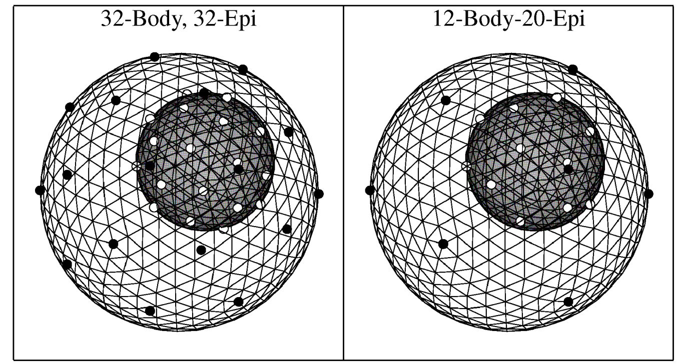

- Telo aproksimiramo s homogeno prevodno kroglo z radijem R=1, ki jo razdelimo na 1280 trikotnikov.
- Površino srca (epikard) pa s kroglo z radijem R_E=0,5 (720 trikotnkov)
- Izbrali smo tri postavitve merskih mest, glej sliko
- Izbrali smo 24 lokacij izvorov (oglišča dveh ikozaedrov – radij očrtane krogle 0.3) V njih smo postavili po tri enojne tokovne dipole vzdolž x,y,z-osi (skupaj 72 izvorov)
- Za dvojne tokovne izvore smo izbrali po12 parov lokacij z majhno (0.179±0.069) srednjo (0.374) in večjo (0.696±0.026) oddaljenostjo. V vsak par lokacij smo postavili po 3 paralelne, anti-paralelne in ortogonalne dvojice dipolov (skupaj 36 izvorov)
- Za vsak enojni in dvojni izvor smo analitično izračunali potenciale na merskih mestih
- Izračunanim mapam smo dodali po 10 naključnih porazdelitev šuma z vrednostmi S/N= 10, 15, 20, 25, 30, 35 in 40 dB.
- S fitanjem (Levenberg-Marquardt) smo iz zašumljenih map določili lego izvorov

Ovrednotenje rezultatov

- Lokalizacijska napaka:

1-dipol $\Delta r = ||\vec{r}_f - \vec{r}_p||_2 \,,$

2-dipola $\Delta r_1, \Delta r_2 \,,\ \Delta r_{\mathrm{c}} = \sqrt{\Delta r_1^2 + \Delta r_2^2}$

- Relativna napaka

$$\mathrm{RE_{fn}} = \frac{||\mathbf{V}_{\mathrm{f}} - \mathbf{V}_{\mathrm{n}}||_2}{||\mathbf{V}_{\mathrm{n}}||_2} \,,\ \mathrm{RE_{fa}} = \frac{||\mathbf{V}_{\mathrm{f}} - \mathbf{V}_{\mathrm{a}}||_2}{||\mathbf{V}_{\mathrm{a}}||_2} \,.$$

Rezultati za enojne dipole

Noise [dB]	32-Body			32-Epi			12-Body-20-Epi		
	$\Delta r/R$±SD	RE_{fn}±SD	RE_{fa}±SD	$\Delta r/R$±SD	RE_{fn}±SD	RE_{fa}±SD	$\Delta r/R$±SD	RE_{fn}±SD	RE_{fa}±SD
10	0.075±0.037	0.283±0.058	0.142±0.048	0.041±0.024	0.300±0.072	0.150±0.059	0.061±0.036	0.291±0.075	0.177±0.073
20	0.023±0.011	0.094±0.019	0.045±0.014	0.012±0.006	0.101±0.026	0.047±0.019	0.018±0.009	0.099±0.027	0.053±0.021
30	0.007±0.004	0.030±0.006	0.014±0.005	0.004±0.002	0.032±0.008	0.015±0.006	0.006±0.003	0.031±0.008	0.018±0.007
40	0.002±0.001	0.009±0.002	0.004±0.002	0.001±0.001	0.010±0.003	0.005±0.002	0.002±0.001	0.010±0.003	0.006±0.002

a)

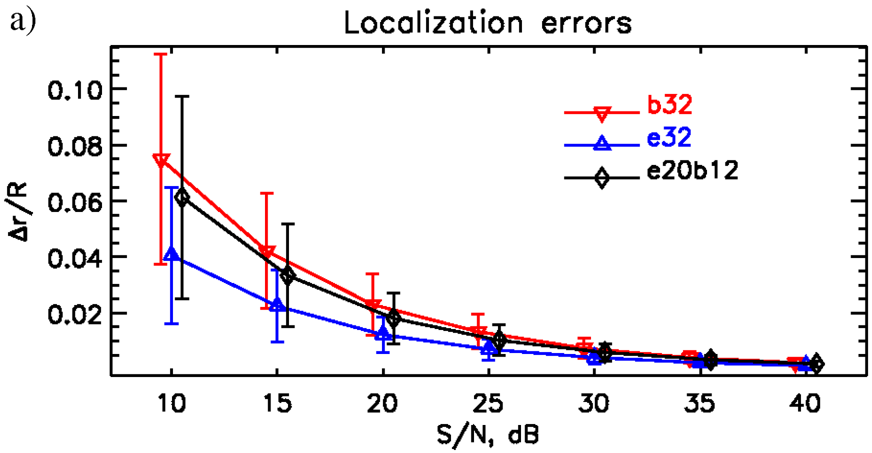

b)

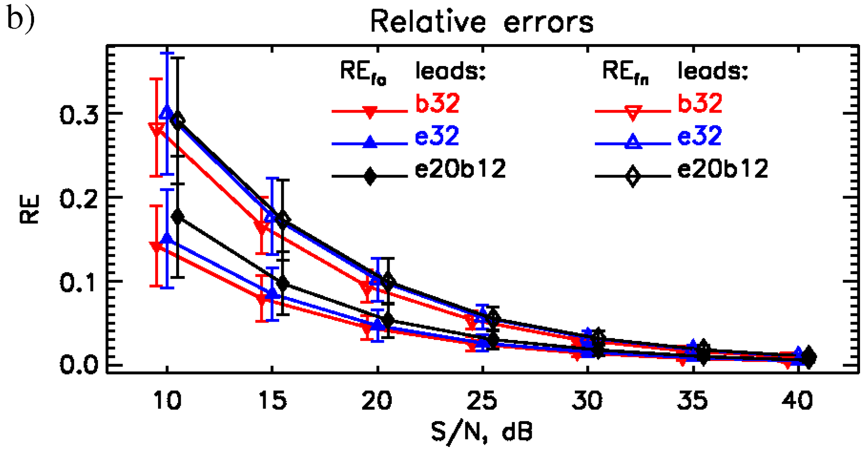

$$S/N = 20\log_{10}\frac{\mathrm{RMS(signal)}}{\mathrm{RMS(noise)}}$$

a)

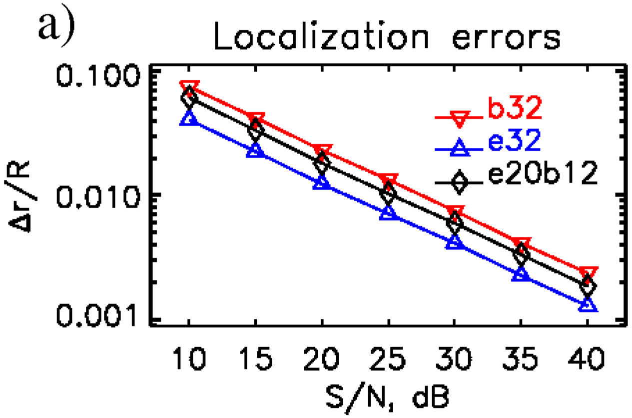

b)

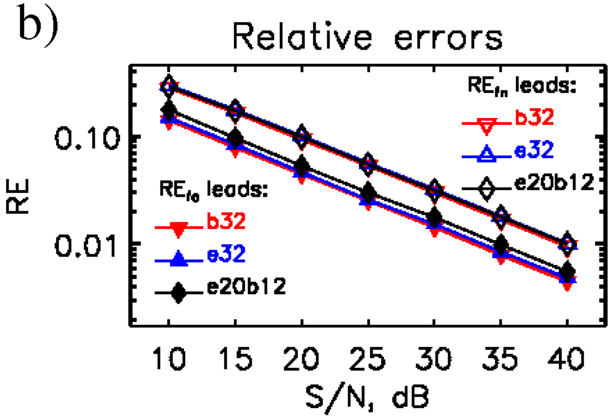

Rezultati za dvojne dipole

	S/N	Parallel dipoles					Anti-parallel dipoles					Perpendicular dipoles				
	[dB]	$\Delta r_1/R$	$\Delta r_2/R$	$\Delta r_c/R \pm SD$	RE_{fn}	RE_{fa}	$\Delta r_1/R$	$\Delta r_2/R$	$\Delta r_c/R \pm SD$	RE_{fn}	RE_{fa}	$\Delta r_1/R$	$\Delta r_2/R$	$\Delta r_c/R \pm SD$	RE_{fn}	RE_{fa}
close	10	0.163	0.162	0.262±0.123	0.223	0.206	0.197	0.204	0.291±0.163	0.590	1.389	0.160	0.161	0.247±0.115	0.300	0.293
close	20	0.093	0.088	0.148±0.116	0.077	0.063	0.081	0.080	0.117±0.114	0.346	0.409	0.063	0.060	0.096±0.083	0.108	0.086
close	30	0.033	0.031	0.051±0.077	0.025	0.020	0.029	0.029	0.042±0.047	0.149	0.128	0.022	0.021	0.033±0.034	0.034	0.027
close	40	0.013	0.013	0.021±0.058	0.008	0.006	0.009	0.008	0.012±0.013	0.050	0.038	0.007	0.007	0.010±0.010	0.011	0.008
median	10	0.116	0.101	0.166±0.086	0.199	0.177	0.122	0.086	0.156±0.074	0.363	0.345	0.117	0.086	0.152±0.068	0.249	0.229
median	20	0.033	0.031	0.048±0.026	0.068	0.054	0.030	0.030	0.045±0.022	0.134	0.106	0.030	0.026	0.042±0.018	0.088	0.067
median	30	0.010	0.013	0.018±0.019	0.022	0.017	0.010	0.010	0.015±0.009	0.043	0.032	0.009	0.008	0.013±0.009	0.028	0.021
median	40	0.003	0.003	0.005±0.003	0.007	0.005	0.003	0.003	0.005±0.004	0.013	0.011	0.003	0.003	0.004±0.002	0.008	0.007
distant	10	0.061	0.068	0.097±0.044	0.183	0.148	0.051	0.059	0.083±0.037	0.224	0.183	0.055	0.059	0.086±0.039	0.199	0.160
distant	20	0.018	0.021	0.029±0.018	0.059	0.047	0.017	0.021	0.029±0.019	0.075	0.057	0.018	0.021	0.030±0.018	0.065	0.051
distant	30	0.006	0.006	0.009±0.005	0.019	0.015	0.005	0.006	0.009±0.005	0.024	0.018	0.005	0.006	0.008±0.004	0.021	0.016
distant	40	0.002	0.002	0.003±0.001	0.006	0.005	0.002	0.002	0.003±0.001	0.007	0.006	0.002	0.002	0.003±0.001	0.007	0.005

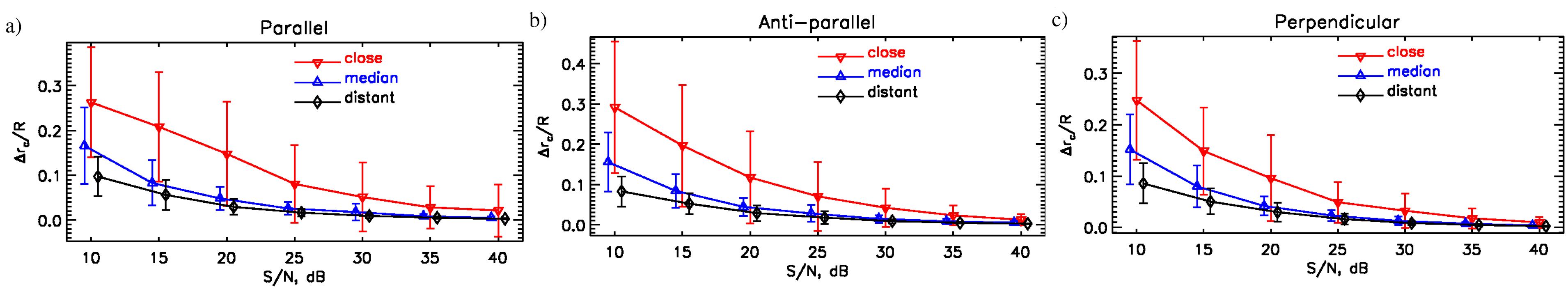

Glavni zaključki

- Merski sistemi postavljeni bližje izvorom so učinkovitejši.
- Za visoke S/N vrednosti gredo lokalizacijske napake proti nič tako za enojne kot dvojne izvore.
- Lokalizacija dvojnih izvorov je odvisna od razdalje med njima, medtem ko medsebojna orientacija nima pomembnega vpliva.

Hvala za pozornost

Položaji izvorov

Enojni dipoli

Table 1: Relative positions of nodes of the 1st and the 2nd icosahedron inside body surface ($\rho_B = r_p/R_B$, outer sphere with radius $R_B = R = 1$) positioned in the center of Cartesian coordinate system and inside epicard surface ($\rho_E = ||\vec{r}_p - \vec{r}_E||/R_E$, inner sphere with radius $R_E = 0.5$) shifted by $\vec{r}_E = (0.1, -0.2, 0.3)$. Both icosahedrons have same dimension defined by circumsribed sphere radius of 0.3.

1st icosahedron			2nd icosahedron		
N_1	ρ_B	ρ_E	N_2	ρ_B	ρ_E
1	0.340	0.078	1	0.714	0.681
2	0.340	0.418	2	0.684	0.681
3	0.210	0.482	3	0.557	0.421
4	0.400	0.388	4	0.750	0.800
5	0.210	0.494	5	0.554	0.421
6	0.340	0.441	6	0.680	0.681
7	0.340	0.683	7	0.628	0.681
8	0.210	0.719	8	0.489	0.421
9	0.000	0.748	9	0.374	0.000
10	0.340	0.692	10	0.626	0.681
11	0.210	0.732	11	0.484	0.421
12	0.210	0.840	12	0.438	0.421

Dvojni dipoli

Table 2: Pairs (N_1,N_2) of positions from the 1st and the 2nd icosahedron (see, Table 1) used for dual dipoles sources.

close (0.178±0.069)		median(0.374)		distant(0.696±0.026)	
(N_1,N_2)	Δr_{12}	(N_1,N_2)	Δr_{12}	(N_1,N_2)	Δr_{12}
(1,9)	0.039	(1,1)	0.374	(9,4)	0.745
(4,12)	0.039	(2,2)	0.374	(12,1)	0.739
(2,8)	0.165	(3,3)	0.374	(9,1)	0.714
(6,11)	0.165	(4,4)	0.374	(12,4)	0.714
(4,9)	0.194	(5,5)	0.374	(9,2)	0.684
(2,9)	0.209	(6,6)	0.374	(11,4)	0.684
(4,11)	0.209	(7,7)	0.374	(8,4)	0.680
(4,8)	0.220	(8,8)	0.374	(9,6)	0.680
(6,9)	0.220	(9,9)	0.374	(11,2)	0.680
(1,11)	0.227	(10,10)	0.374	(11,1)	0.678
(2,12)	0.227	(11,11)	0.374	(12,2)	0.678
(1,5)	0.230	(12,12)	0.374	(8,1)	0.675

A Appendix: Analytical solution

Electric potential on a surface and within a conducting sphere with radius R generated by an arbitrary dipole $\vec{p}$ at location $\vec{r}_p$ anywhere ($\vec{r} \neq \vec{r}_p$) within the sphere can be solved analytically by a closed solution derived by Yao[2]

$$V(\vec{r}) = \frac{\vec{p}}{4\pi\sigma R^3} \cdot \left\{ \frac{R^3(\vec{r}-\vec{r}_p)}{|\vec{r}-\vec{r}_p|^3} + \frac{1}{r_{pi}^3}\left(\vec{r} - \frac{r^2}{R^2}\vec{r}_p\right) + \frac{1}{r_{pi}}\left[\vec{r} + \frac{(\vec{r}\cdot\vec{r}_p)\vec{r} - r^2\vec{r}_p}{R^2(r_{pi}+1)-(\vec{r}\cdot\vec{r}_p)}\right]\right\}, \quad (5)$$

where $r = |\vec{r}|$, $r_p = |\vec{r}_p|$ and

$$r_{pi} = \left[1 + \left(\frac{r_p r}{R^2}\right)^2 - 2\frac{(\vec{r}\cdot\vec{r}_p)}{R^2}\right]^{1/2}. \quad (6)$$

Note, that in the original formula (Eq. (13) in [2]), the $(\vec{r}\cdot\vec{r}_p)$ is expressed as $(r_p r\cos\varphi)$, where φ is the angle between $\vec{r}$ and $\vec{r}_p$. For the surface potential, $r \equiv R$, $Rr_{pi} = |\vec{R} - \vec{r}_p|$, Eq. (1) is simplified to

$$V(\vec{R}) = \frac{\vec{p}}{4\pi\sigma R^3} \cdot \left\{ 2\frac{R^3(\vec{R}-\vec{r}_p)}{|\vec{R}-\vec{r}_p|^3} + \frac{R}{|\vec{R}-\vec{r}_p|}\left[\vec{R} + \frac{(\vec{R}\cdot\vec{r}_p)\vec{R} - R\vec{r}_p}{|\vec{R}-\vec{r}_p| + R - r_p\cos\varphi}\right]\right\}, \quad (7)$$

which is the same as the formula derived by Brody et al. [3]. For a special case, when the current dipole is in the center of the conducting sphere ($r_p = 0$), we get well known result $V(\vec{R}) = 3\frac{\vec{p}\cdot\vec{R}}{4\pi\sigma R^3} = 3V_\infty(\vec{R})$, where V_∞ is the potential generated by the current dipole source in an infinite conducting space.

The general solution (5) can be re-arranged in the following form, which is more suitable for applying it in computer programmes and calculating derivatives

$$V(\vec{r}) = \frac{1}{4\pi\sigma R^3}\left[f(\vec{r})(\vec{p}\cdot\vec{r}) - g(\vec{r})(\vec{p}\cdot\vec{r}_p)\right], \quad (8)$$

where

$$f(\vec{r}) = \frac{R^3}{|\vec{r}-\vec{r}_p|^3} + \frac{1}{r_{pi}}\left[1 + \frac{1}{r_{pi}^2} + \frac{(\vec{r}\cdot\vec{r}_p)}{R^2(r_{pi}+1)-(\vec{r}\cdot\vec{r}_p)}\right] = f_1(\vec{r}) + \frac{1 + f_2(\vec{r}) + f_3(\vec{r})}{r_{pi}}, \quad (9)$$

and

$$g(\vec{r}) = \frac{R^3}{|\vec{r}-\vec{r}_p|^3} + \frac{1}{r_{pi}}\left[\frac{1}{r_{pi}^2}\frac{r^2}{R^2} + \frac{r^2}{R^2(r_{pi}+1)-(\vec{r}\cdot\vec{r}_p)}\right] = g_1(\vec{r}) + \frac{g_2(\vec{r}) + g_3(\vec{r})}{r_{pi}}, \quad (10)$$

where $f_1(\vec{r}) = g_1(\vec{r}) = \frac{R^3}{|\vec{r}-\vec{r}_p|^3}$, $f_2(\vec{r}) = \frac{1}{r_{pi}^2}$, $f_3(\vec{r}) = \frac{\vec{r}\cdot\vec{r}_p}{D}$, $g_2(\vec{r}) = \frac{r^2}{R^2}f_2(\vec{r})$, $g_3(\vec{r}) = \frac{r^2}{D}$, and $D = R^2(r_{pi}+1) - \vec{r}\cdot\vec{r}_p$.

During nonlinear least square fitting procedures, when we are looking for the optimal source parameters, i.e. dipole location $\vec{r}_p$ and dipole strength $\vec{p}$, we need also partial derivatives over those parameters that can be expressed as

$$\nabla_p V = \left(\frac{\partial V}{\partial x_p}, \frac{\partial V}{\partial y_p}, \frac{\partial V}{\partial z_p}\right) \text{ and } \nabla_s V = \left(\frac{\partial V}{\partial p_x}, \frac{\partial V}{\partial p_y}, \frac{\partial V}{\partial p_z}\right), \quad (11)$$

where ∇_p and ∇_s represent gradients of source location and source strength, respectively. Gradient of potential (8) can be generally expressed as

$$\nabla V(\vec{r}) = \frac{1}{4\pi\sigma R^3}\Big[f(\vec{r})\nabla(\vec{p}\cdot\vec{r}) + (\vec{p}\cdot\vec{r})\nabla f(\vec{r}) - f(\vec{r})\nabla(\vec{p}\cdot\vec{r}_p) - (\vec{p}\cdot\vec{r}_p)\nabla g(\vec{r})\Big]. \quad (12)$$

Components of source strength are included only in $(\vec{p}\cdot\vec{r})$ and $(\vec{p}\cdot\vec{r}_p)$, what leads to

$$\nabla_s V(\vec{r}) = \frac{1}{4\pi\sigma R^3}\left[f(\vec{r})\vec{r} - g(\vec{r})\vec{r}_p\right], \quad (13)$$

and the potential in (8) can be written as

$$V(\vec{r}) = \vec{p}\cdot\nabla_s V(\vec{r}). \quad (14)$$

The above formula can be used in linear least square fitting procedures [5], where the source location is known and only the source sthregth has to be determined.

On the other hand, components of source coordinates $\vec{r}_p$ are also included in $f(\vec{r})$, $g(\vec{r})$ and r_{pi}. Consequently, non-linear least square, like the Levengerg-Marquardt algoritm [5], has to be applied in the fitting procedure. From (8) and (12) it follows

$$\nabla_p V = \frac{1}{4\pi\sigma R^3}\left[(\vec{p}\cdot\vec{r})\nabla_p f - g\,\vec{p} - (\vec{p}\cdot\vec{r}_p)\nabla_p g\right], \quad (15)$$

where $\nabla_p f$ and $\nabla_p g$ are

$$\nabla_p f = \nabla f_1 + \frac{\nabla f_2 + \nabla f_3}{r_{pi}} - \frac{\nabla r_{pi}}{r_{pi}^2}(1 + f_2 + f_3) \quad (16)$$

$$\nabla_p g = \nabla g_1 + \frac{\nabla g_2 + \nabla g_3}{r_{pi}} - \frac{\nabla r_{pi}}{r_{pi}^2}(g_2 + g_3), \quad (17)$$

where $\nabla_p f_1 = \nabla_p g_1 = 3R^3\frac{\vec{r}-\vec{r}_p}{|\vec{r}-\vec{r}_p|^5}$, $\nabla_p f_2 = -2\frac{\nabla_p r_{pi}}{r_{pi}^3}$,

$\nabla_p f_3 = \frac{\vec{r}}{D} - (\vec{r}\cdot\vec{r}_p)\frac{\nabla_p D}{D^2}$, $\nabla_p g_2 = \frac{r^2}{R^2}\nabla_p f_2$, $\nabla_p g_3 = -r^2\frac{\nabla_p D}{D^2}$,

$\nabla_p r_{pi} = \frac{1}{R^2 r_{pi}}\left[\frac{r^2}{R^2}\vec{r} - \vec{r}\right]$, $\nabla_p D = R^2\nabla_p r_{pi} - \vec{r}_p$.

References

[1] R. Hren, G. Stroink, B.M. Horáček: Accuracy of single-dipole inverse solution when localising ventricular pre-excitation sites: simulation study. *Med. Biol. Eng. Comp.*, **36**:323-9, 1998.

[2] D. Yao: Electric Potential Produced by a Dipole in a Homogeneous Conducting Sphere. *IEEE Trans. Biomed. Eng.*, vol. BME-44, pp. 964-6, Jul. 2000.

[3] D. A. Brody, F. H. Terry, and R. E. Ideker: Eccentric dipole in a spherical medium: generalized expression for surface potentials. *IEEE Trans. Biomed. Eng.*, vol. BME-20, pp. 141–3, Mar. 1973.

[4] M. Milanič, V. Jazbinšek, R. Hren: Assessment of regularization techniques used in solving the ill-posed inverse problem of electrocardiography. In B. Zajc, A. Trost: Proceedings of 18th Electrotechnical and Computer Science Conference ERK 2009, 21. - 23. September 2009, Portorož, Slovenija

[5] W.H. Press, B.P. Flannery, S.A. Teukolsky,W.T. Vetterling. Numerical Recipes - The Art of Scientific Computing, Cambridge University Press, 1989.